Materials Science-Poland, 37(2), 2019, pp. 182-189
http://www.materialsscience.pwr.wroc.pl/
DOI: 10.2478/msp-2019-0017

sciendo

Ab initio study of $GdCo_5$ magnetic and magneto-optical properties

M. MAHDI[1,*], A. DJABRI[1], M. M. KOC[2], R. BOUKHALFA[1], M. ERKOVAN[3], YU. CHUMAKOV[4], F. CHEMAM[1]

[1]Laboratory of Applied and Theoretical Physics, Laarbi Tebessi University, Tebessa, Algeria
[2]Department of Physics, Kirklareli University, Kirklareli, Turkey
[3]Nanoscience and Nanotechnology Dept. Sakarya University, Sakarya, Turkey
[4]Department of Physics, Gebze Technical University, Cayırova, Kocaeli-Turkey

The full potential linearized augmented plane wave method (FLAPW) including the spin-orbit coupling has been used to study the structural, electronic and magnetic properties of $GdCo_5$ compound. The calculations were performed within the local spin density approximation (LSDA) as well as Coulomb corrected LSDA + U approach. The study revealed that the LSDA + U method gave a better representation of the band structure, density of states and magnetic moments than LSDA. It was found that the spin magnetic moment of Co (2c) and Co (3g) atoms in the studied compound is smaller compared to the one in bulk Co. The optical and magneto-optical properties and the magneto-optical Kerr effect have also been investigated.

Keywords: *ab initio calculations; magnetic moment; spin orbit coupling; spin polarization; magneto-optical Kerr effect*

1. Introduction

Magnetic and electronic properties of intermetallic compounds which contain rare earth (RE) and transition metal (TM) elements, are of significant importance. They are crucial in numerous commercial and industrial applications, including high-power, high-temperature permanent magnets, microwave devices with improved performance, biomedical materials for medical sensors, fuel for heterogeneous catalysts, and many other applications.

New magnetic materials attract the attention of researchers because of their unusual intrinsic magnetic properties, such as significant magnetic moment, high magneto-crystalline anisotropy and high Curie temperatures [1–3]. The studies have shown that magnetic properties of the materials are related to the electronic configuration of their atoms.

It was found that 4f states form a subset of localized magnetic moments, while the 3d TM ones are responsible for metallic bonding and magnetic ordering. These states are considered as nearly free states participating in the bonding in the presence of 4s TM and 5d RE states [4, 5].

For many years, researchers have been studying rare earth/transition metal (RE/TM) compounds, including the electronic properties of $GdFe_2$, $GdCo_2$, $(Y,Gd)Co_2$, YCo_2, La_2Co_7 [6–9], and the magneto-optical properties of different RE/TM compounds like $GdFe_2$, $HoFe_2$, $ErFe_2$, $TbFe_2$, $DyFe_2$ and YFe_2 [10, 11]. A magnetocaloric effect was studied in $GdCo_5$ alloys which exhibit magnetic phase transition near the room temperature [12]. Large magnetic anisotropy and perpendicular orientation of magnetic moment were observed in $GdCo_5$ [13]. The temperature dependence of magnetic anisotropy was determined for $GdCo_5$ and YCo_5 by introducing the first-principles approach to calculate temperature-dependent magnetization versus field (FPMVB) [14]. This approach solves the problem of the large value of magnetocrystalline anisotropy of $GdCo_5$ at 0 K.

*E-mail: mouh2009@gmail.com

This work highlights the electronic, magnetic and magneto-optical Kerr effect properties of $GdCo_5$ based on the first principles calculations, using LSDA and LSDA + U methods.

2. Computational methods

First principle calculations were performed using the relativistic all-electron full potential linearized augmented plane wave (FPLAPW) method implemented in the WIEN2k code version 14.1 [15]. The local spin density approximation (LSDA) functional [16] and LSDA + U applied to the 4f electrons [17] were employed in this work.

It is known that LSDA may lead to a relatively incorrect prediction of magnetic properties. Therefore, we used LSDA + U calculations with a spin-orbit coupling (SOC) to distinguish different properties of the compound (e.g. ferrimagnetic vs. ferromagnetic) [17, 18]. In LSDA + U calculations, we have used an onsite Coulomb interaction with U = 6.7 eV and an exchange parameter J = 0.7 eV [19] for the Gd (4f) electrons. $GdCo_5$ have a $CaCu_5$ type structure (P6/mmm, space group No. 191). The experimental values of a and c/a used in the calculation were 4.963 Å and 0.801 Å, respectively [20]. The Gd and Co atom positions are summarized in Table 1. A mesh of 793 k points in the irreducible part of the Brillouin zone has been used for $GdCo_5$. A denser mesh of 2052 k points in the irreducible part of the Brillouin zone has been chosen for the investigation of the magneto-optical (MO) properties. The radii of the muffin-tin spheres are equal to 2.3 and 2.5 for Co and Gd, respectively. The cut-off parameters are $R_{MT} \cdot K_{max} = 7$ for the plane wave and $R_{MT} \cdot G_{max} = 12$ for the charge density, K_{max} represents the maximum wave number of the plane wave in the interstitial region, and G_{max} is the maximum reciprocal lattice vector. The criterion for total energy convergence is 0.0001 Ry and the default value of the energy separation between core/valence is −6.0 Ry.

Table 1. Lattice constants and atomic positions (x y z) of $GdCo_5$ [20].

GdCo5	
a [Å]	4.963
c [Å]	3.973
atoms	positions
Gd	(0 0 0)
Co1 (2c)	(1/3 2/3 0)
Co2 (3g)	(1/2 0 1/2)

3. Results and discussion

3.1. Magnetic properties

The calculated spin magnetic moments, based on experimental geometry, are shown in Table 2. The previous calculations made by both LSDA and LSDA + U methods proved that Gd and Co magnetic moments are antiparallel to each other [2, 5]. Thus, the band structure and density of states (DOS) were calculated to better understand the magnetic properties of $GdCo_5$ (Fig. 1a and Fig. 1b).

Within LSDA + U approach, it was found that the strongest DOS peaks for the majority spins are located at −7 eV below the Fermi level, while for minority spins the peaks are located at 4 eV above it. These peaks consist of the Gd (4f) state. For minority spins, this state is hybridized with d and p bands of Co, while it is unhybridized in the case of majority spins [6].

The f band in LSDA approximation is located at −4 eV for the spin up and 1 eV for spin down. Thus, it is shifted towards higher binding energies for the spin up and towards the positive energies for the spin down (Fig. 1c and Fig. 1d).

The DOS width of the Gd (4f) state in the $GdCo_5$ compound calculated by LSDA + U method is equal to 0.5 eV for both majority and minority spins. This value is comparable to that of an isolated Gd atom. The exchange coupling has significantly been enhanced with the introduction of the Hubbard parameter U.

The calculated spin magnetic moments and the density of states (DOS) at Fermi level E_F are presented in Table 2. The spin magnetic moments

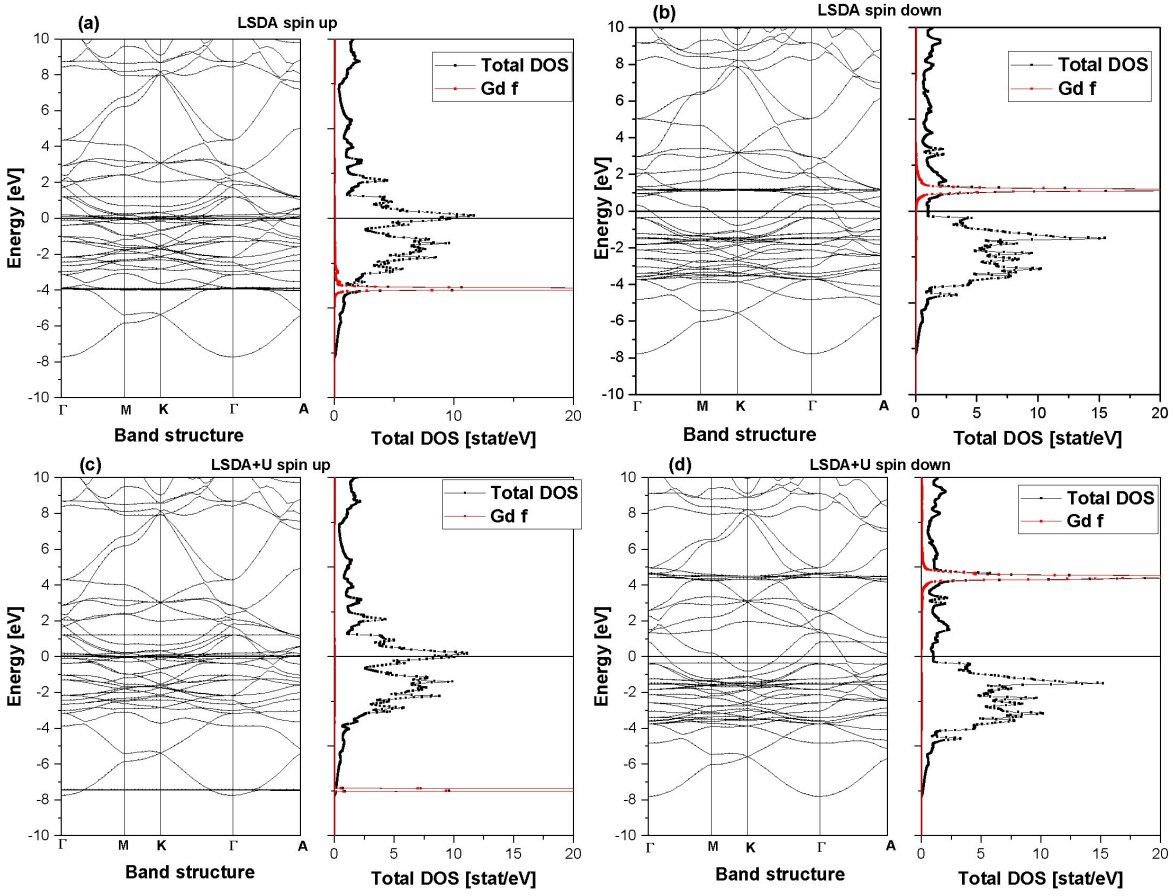

Fig. 1. (a) band structure and total density of states for LSDA spin up, (b) band structure and total density of states for LSDA spin down, (c) band structure and total density of states for LSDA + U spin up, (d) band structure and total density of states for LSDA + U spin down.

of Gd atom in $GdCo_5$ are equal to 7.32 μ_B and 7.07 μ_B for LSDA + U and LSDA, respectively. In this compound we observed a reduction in the spin magnetic moment of Co (Table 2) due to the filling of the minority spin d states through hybridization, which explains the increase of Co (3d) magnetic moments in $GdCo_5$ in comparison with pure Co.

The contributions of Co (3g) and Co (2c) atoms to the spin magnetic moment are 1.89 μ_B, 1.77 μ_B for LSDA + U and 1.58 μ_B, 1.54 μ_B for LSDA calculations. Hund's rule suggests that Gd has a zero orbital magnetic moment so we can neglect it. However, we have calculated it and found that the orbital moment of Gd remains very small (0.03725 μ_B in LSDA + U and 0.00419 μ_B in LSDA + U + SOC). These results are in good agreement with those obtained in previous studies [8, 21]. The cobalt spin magnetic moments have been found to be lower than their experimental values.

Fig. 2 shows the Gd (5d) and Co (3d) contributions in the partial density of state PDOS. According to 4f-5d-3d model [22], the Gd (4f) electrons polarize their 5d bands. There are also Gd (5d) – Co (3d) short-range exchange interactions. The Gd (5d) states are occupied mostly through the 5d-3d hybridization [5], while the localized 4f states are located around 5 eV below the Fermi level. In addition, these states are shifted more to around 7.5 eV if the Coulomb interaction U is added. When the magnetization is parallel to c-axis, the SO interaction will slightly widen the f states.

In the antiparallel orientation calculation, the energy difference before hybridization

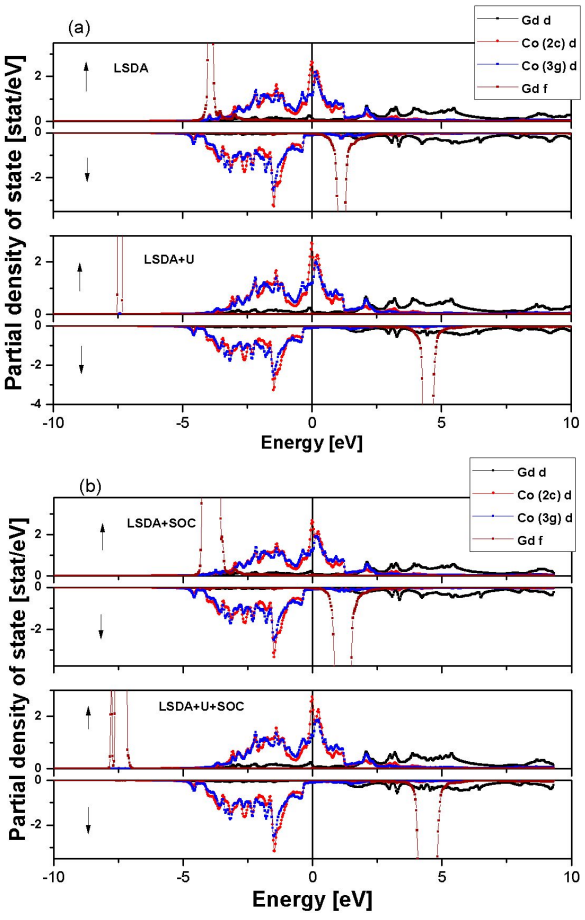

Fig. 2. (a) the calculated partial DOS of $GdCo_5$ without spin-orbit coupling (SOC), (b) the calculated partial DOS of $GdCo_5$ with spin-orbit coupling (SOC). All the calculations were performed within LSDA and LSDA + U. The arrows indicate the spin majority (up) and spin minority (down).

of spin-minority 5d and 3d states will be smaller than the energy difference between 5d and 3d spin-majority states. Also, the 4f-5d intra-atomic exchange interaction will always orient the 5d spin magnetic moments parallel to the 4f spin magnetic moments [5].

The spin polarization at the Fermi level (E_F) is given by the relation [23]:

$$P = \left| \frac{N_\uparrow(E_F) - N_\downarrow(E_F)}{N_\uparrow(E_F) + N_\downarrow(E_F)} \right| \tag{1}$$

where $N_\uparrow(E_F)$ and $N_\downarrow(E_F)$ are the density values for majority and minority spin states, respectively. The values of the spin polarization at the Fermi level are 84.48 % for LSDA + SOC and 85.52 % for LSDA + U + SOC. These large values indicate a strong exchange coupling between Gd (4f) and Co (3d) electrons, which leads to a high magnetocrystalline anisotropy [4].

3.2. Magneto-optical properties

We calculated the dispersion of the optical conductivity tensor $\sigma_{\alpha\beta}(\omega)$, where ω is the frequency of the incoming electromagnetic radiation. The calculation was performed from the energy band structure by means of the Kubo-Greenwood [24, 25] linear response [26]:

$$\sigma_{\alpha\beta}(\omega) = \frac{-ie^2}{m^2 \hbar V_{uc}} \sum_k \sum_{nn'} \frac{f(\varepsilon_{nk}) - f(\varepsilon_{n'k})}{\omega_{nn'}(k)} \frac{\prod^{\infty}_{nn'}(k) \prod^{\beta}_{nn'}(k)}{\omega - \omega_{nn'}(k) + i\gamma} \tag{2}$$

where V_{uc} is the unit-cell volume, $f(\epsilon_{nk})$ is the Fermi function, ϵ_{nk} and $\epsilon_{n'k}$ are the Kohn-Sham energies at the point k for the band n and n′, respectively. $\hbar\omega_{nn'} = \epsilon_{nk} - \epsilon_{n'k}$ is the energy difference for the two bands n and n′, $\prod^{\alpha}_{nn'}(k)$ is the dipolar optical matrix element, $\gamma = \frac{1}{\tau}$ is the lifetime parameter, and τ is the relaxation time parameter.

The imaginary part of the non-diagonal elements of the conductivity tensor describes the magneto-optical absorption. For the polar Kerr effect the magnetization is perpendicular to the surface of the sample and parallel to z-axis.

The dielectric tensor is expressed as:

$$\varepsilon = \begin{pmatrix} \varepsilon_{xx} & \varepsilon_{xy} & 0 \\ -\varepsilon_{xy} & \varepsilon_{xx} & 0 \\ 0 & 0 & \varepsilon_{zz} \end{pmatrix} \tag{3}$$

where ϵ_{xx} and ϵ_{zz} are the diagonal components and ϵ_{xy} the off-diagonal component of the dielectric tensor. The optical conductivity tensor $\sigma_{\alpha\beta} = \sigma^{(1)}_{\alpha\beta} + \sigma^{(2)}_{\alpha\beta}$ is related to the dielectric tensor by the equation:

$$\varepsilon_{\alpha\beta}(\omega) = \delta_{\alpha\beta} + \frac{4\pi i}{\omega} \sigma_{\alpha\beta}(\omega) \tag{4}$$

Table 2. Spin magnetic moments calculated in the antiferromagnetic configurations for $GdCo_5$ and spin magnetic moments of Gd and Co (μ_B). The calculated DOS at Fermi level E_F for majority and minority spin.

System	$N_\uparrow(E_F)$	$N_\downarrow(E_F)$	P %	μ_{Gd}	μ_{Co}	μ_{Co}^{2c}	μ_{Co}^{3g}	μ_{Total}
LSDA + U								
Gd	0.98	2.97	50.37	7.04	–	–	–	7.04
Co	0.33	1.78	68.78	–	1.74	–	–	1.74
$GdCo_5$	1.05	9.83	80.7	7.32	–	–1.77	–1.89	–0.97
LSDA								
Gd	1.01	1.24	10.2	6.93	–	–	–	6.93
Co	0.24	1.65	74.60	–	1.71	–	–	1.71
$GdCo_5$	1.7	0.76	38.20	7.07	–	–1.54	–1.58	–0.20
LSDA + U + SOC								
Gd	1.76	9.27	67.97	6.72	–	–	–	6.72
Co	0.30	1.65	68.61	–	2.18	–	–	2.18
$GdCo_5$	12.30	0.96	85.52	7.02	–	–1.48	–1.51	–0.40
LSDA + SOC								
Gd	1.38	3.29	40.74	7.06	–	–	–	7.06
Co	0.37	1.48	59.74	–	1.63	–	–	1.63
$GdCo_5$	12.6	1.06	84.48	6.84	–	–1.46	–1.49	–0.47

For the linear polarization, the solution of Maxwell equation gives the relation between the complex Kerr angle and the dielectric tensor. Assuming that θ_k and ϵ_k are small, they are given by the following relations [27, 28]:

$$\varphi_k = \theta_k + i\varepsilon_k \tag{5}$$

$$\theta_k + i\varepsilon_k = \frac{-\sigma_{xy}}{\sigma_{xx}\sqrt{1+\left(\frac{4\pi i}{\omega}\right)\sigma_{xx}}} \tag{6}$$

where θ_k is the Kerr rotation and ε_k the Kerr ellipticity.

In order to study the magneto-optical behavior of the system, the spectral calculation of the Kerr effect in polar geometry has been performed (P-MOKE).

It is known that the magneto-optical effect originates from interband and intraband transitions. The intraband transition of 3d transition metals or 5d rare earth and the interband d-f or d-p contribute to the Kerr rotation spectra [29]. Generally, the net spin polarization, the spin-orbit coupling and even the density of states near the Fermi level are important factors contributing to the magnitude of the Kerr effect, which is determined by the off-diagonal components of the conductivity tensor.

Fig. 3 shows the diagonal and off-diagonal optical conductivity ($\sigma_{xx}(\omega)$ and $\sigma_{xy}(\omega)$) for the compound calculated using both LSDA+SOC and LSDA + U + SOC methods with spin-orbit coupling and the broadening of 0.7 eV. The most suitable broadening parameter can be chosen by trying different values and comparing their relative sharpness. A small value of the broadening indicates weaker scattering. Fig. 3a and Fig. 3b show the absorption curve σ_{xx}^1 and the dispersive part σ_{xx}^2 of optical conductivity in the range of 0 to 14 eV. The curves obtained by both methods are very similar. In the 1 eV to 6 eV energy range, the corresponding peaks are practically at the same positions, but the magnitude of the peak is higher in the framework of LSDA + SOC. The two peaks are the strongest and originate from the p-d interband transition [29, 30] located around 2 eV and 5.5 eV. The third peak is located around 9 eV.

The off-diagonal conductivity curves (Fig. 3c and Fig. 3d) $\sigma_{xy}(\omega)$ and $\omega \cdot \sigma_{xy}(\omega)$ (Fig. 3e)

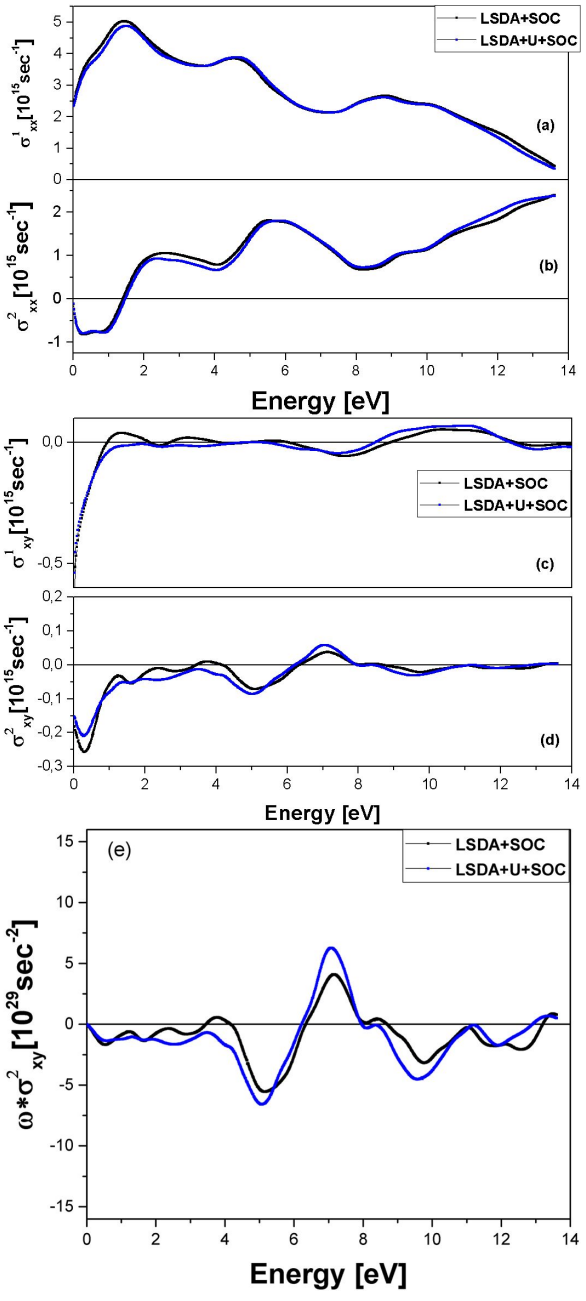

Fig. 3. (a) and (b) absorption optical conductivity $\sigma^1_{xx}(\omega)$ and the dispersive $\sigma^2_{xx}(\omega)$ part; (c) and (d) calculated real off-diagonal $\sigma^1_{xy}(\omega)$ and imaginary off-diagonal $\sigma^2_{xy}(\omega)$; (e) off-diagonal optical conductivity $\omega.\sigma^2_{xy}(\omega)$.

carry information about the Kerr rotation and ellipticity. The obtained result is also proportional to the difference in the absorption rate of the left and right circularly polarized light (LCP and RCP) [31, 32]. Its sign is directly related to the spin polarization of the states responsible for the interband transitions producing the structures in the spectrum.

In order to find the origin of the studied Kerr spectra, it is useful to consider the absorptive part of the off-diagonal optical conductivity $\sigma^2_{xy}(\omega)$, since it plays an important role in Kerr effect (equation 6). When comparing $\omega \cdot \sigma^2_{xy}(\omega)$ with the Kerr rotation, it was found that the signature of σ^2_{xy} dependence is stronger than the σ^1_{xx} dependence [29].

It is interesting to note that the $\omega \cdot \sigma^2_{xy}(\omega)$ spectrum and the Kerr rotation in Fig. 3e and Fig. 4a have a similar line shape. The numbers of dominant and prominent peaks are equal in both spectra.

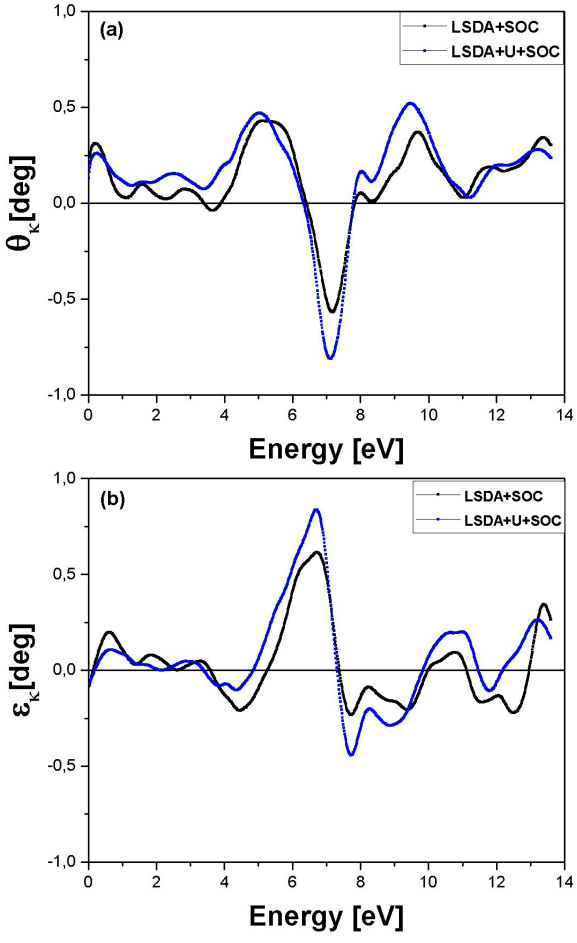

Fig. 4. Calculated (a) Kerr angle and (b) Kerr ellipticity.

Fig. 4 shows the Kerr rotation and ellipticity. The two graphs are related to each other. A zero

value in ellipticity corresponds to a peak in the Kerr rotation [32]. A vanishing ellipticity means that the light waves remain linearly polarized at these frequencies [33]. In LSDA + U + SOC we observe a main peak of 0.5° located at 5 eV having a large width of 1.5 eV, a second peak of −0.7° located at 7 eV and another peak of 0.5° at 9.5 eV. For LSDA + SOC we found a similar structure with smaller angles. The two main peaks are located at 5.5 eV and 7 eV, and a weaker peak is located at an energy range greater than 10 eV.

4. Conclusions

The full potential linear augmented plane wave method including the spin-orbit coupling has been used to study the structural, electronic and magnetic properties of the $GdCo_5$ compound. The calculations were made within the local spin density approximation LSDA and Coulomb corrected local spin density approximation LSDA + U. It was found that the value of magnetic moment is in agreement with the experimental results within the LSDA + U approximation. The hybridization of the minority spin d states of Co in $GdCo_5$ leads to a decrease in the Co magnetic moment. The contributions of Co(3g) and Co(2c) atoms to the spin magnetic moment are (1.89 μ_B, 1.77 μ_B) and (1.58 μ_B, 1.54 μ_B) for LSDA + U and LSDA calculations, respectively. It was also observed that the values of $Re\sigma_{xx}(\omega)$ obtained by LSDA + SOC and LSDA + U + SOC methods are very similar and the corresponding peaks are practically at the same position but the magnitude of the peaks in the case of the LSDA + SOC method is higher.

References

[1] BUSCHOW K.H.J., *Rep. Prog. Phys.*, 40 (1977), 1179.
[2] MILETIC G.I., BLAZINA Z., *J. Magn. Magn. Mater.*, 321 (2009), 3888.
[3] LIEBS M., HURNMLER K., FAHNLEE M., *Phys. Rev. B*, 46 (1992), 11201.
[4] RICHTER M., *J. Phys. D Appl. Phys.*, 31 (1998), 1017.
[5] MILETIC G.I., BLAZINA Z., *J.Magn. Magn. Mater.*, 284 (2004), 312.
[6] SAINI S.M., SINGH N., NAUTIYAL T., AULUCK S., *J. Phys. Cond. Mater.*, 19 (2007), 176203.
[7] ŚNIADECKI Z., WERWIŃSKI M., SZAJEK A., RÖSSLER U.K., IDZIKOWSKI B., *J. Appl Phys.*, 115 (2014), 17E129.
[8] PIERUNEK N., ŚNIADECKI Z., WERWIŃSKI M., WASILEWSKI B., FRANCO V., IDZIKOWSKI B., *J. Alloy. Compd.*, 702 (2017), 258.
[9] KUZ'MIN M.D., SKOKOV K.P., RADULOV I., SCHWÖBEL C.A., FORO S., DONNER W., WERWIŃSKI M., RUSZ J., DELCZEG-CZIRJAK E., GUTFLEISCH O., *J. Appl. Phys.*, 118 (2015), 053905.
[10] KRAVETS V.G., POPERENKO L.V., SHAIKEVICH I.A., *Soviet Phys. J.*, 31 (1988), 1007.
[11] SHARIPOV SH.M., MUKIMOV K.M., ERNAZAROVAL A., ANDEREYEV A.V., KUDERVATYKH N.V., *Phys. Met. Metall.*, 69 (1990), 50.
[12] NIKITIN S.A., BOGDANOV A.E., MOROZKIN A.V., KNOTKO A.V., YAPASKURT V.O., OVCHENKOVA I.A., SMIRNOV A.V., NIRMALA R., QUEZADO S., MALIK S.K., *Mater. Res. Express*, 5 (2018), 036109.
[13] FUTAMOTO M., OHTAKE M., *Jpn. J. Magn. Soc.*, 41 (2017), 108.
[14] PATRICK C.E., KUMAR S., BALAKRISHNAN G., EDWARDS R.S., LEES M.R., PETIT L., STAUNTON J.B., *Phys. Rev. Lett.*, 120 (2018), 097202.
[15] BLAHA P., MADSEN G., SCHWARZ K., KVASNICKA D., LUITZ J., *WIEN2k: An Augmented Plane Wave plus Local Orbitals Program for Calculating Crystal Properties*, TU Vienna, Austria, 2001.
[16] PERDEW J.P., WANG Y., *Phys. Rev. B*, 45 (1992), 13244.
[17] ANISIMOV V.I., ARYASETIAWAN F., LICHTENSTEIN A.I., *J. Phys-Condens. Mater.*, 9 (1997), 767.
[18] YEHIA S., ALY S.H., ALY A.E., *Comput. Mater. Sci.*, 41 (2008), 482.
[19] HARMON B.N., ANTROPOV V.P., LICHTENSTEIN A.I., SOLOVYEV I.V., ANISIMOV V. I., *J. Phys. Chem. Solids*, 56 (1995), 1521.
[20] IDO H., NANJO M., YAMADA M., *J. Appl. Phys.*, 75 (1994), 7140.
[21] HUMMLER K., FAHNLE M., *Phys. Rev. B*, 53 (1996), 3272.
[22] CAMPBELL I.A., *J. Phys. F. Metal. Phys.*, 2 (1972), L47.
[23] HIROHATA A., TAKANASHI K., *J. Phys. D Appl. Phys.*, 47 (2014), 193001.
[24] ZHANG H., RICHTER M., KOEPERNIK K., OPAHLE I., TASNADI F., ESCHRIG H., *New J. Phys.*, 11 (2009), 043007.
[25] GRUNDY P.J., *Mater. Sci. Technol. B*, 3 (1994), 568.
[26] KUBO R., *Jpn. J. Phys. Soc.*, 12 (1957), 570.
[27] KUBO J., *Jpn. J. Phys. Soc.*, 12 (1972), 570.
[28] WANG C.S., CALLAWAY J., *Phys. Rev. B*, 9 (1974), 4897.
[29] ERSKINE J.L., *AlP Conf. Frec.*, 24 (1975), 190.
[30] KUMAR M., NAUTIYAL T., AULUCK S., *Eur. Phys. J. B*, 73 (2010), 423.
[31] HANSEN P., CLAUSEN C., MUCH G., ROSENKRANZ M., WITTER K., *J. Appl. Phys.*, 66 (1989), 756.
[32] CAI J., TAO X.A., CHEN W., ZHAO X., TAN M., *J. Magn. Magn. Mater.*, 292 (2005), 476.

[33] WEN H., KAWAZOE Y., DONG J., *Phys. Rev. B*, 74 (2006), 085205.

Received 2018-02-20
Accepted 2018-05-21